2B.4 SENSITIVITY OF VERTICAL STRUCTURE IN THE STABLE BOUNDARY LAYER TO VARIATIONS OF THE WRF MODEL'S MELLOR-YAMADA-JANJIC TURBULENCE SCHEME

Nelson L. Seaman[1]*, Brian J. Gaudet[1], Jeff Zielonka[1] and David R. Stauffer[1]

[1]Pennsylvania State University, University Park, Pennsylvania

1. INTRODUCTION

Very stable boundary layers with shallow depths (often only tens of meters) present a serious challenge for mesoscale models, including WRF. Errors in meteorological forecasts of wind speed and direction, thermal inversion strength, and depth of the stable boundary layer (SBL) can have serious consequences for atmospheric transport and dispersion (AT&D) predictions and for other air-quality applications.

In very stable conditions, buoyancy forces strongly suppress vertical motions, so SBL wind fluctuations are limited mostly to the horizontal. When synoptic forcing is weak and mean flow is light (~2 ms^{-1} or less), wind fluctuations often have the same magnitude as the mean speed. In this case transport can become erratic due to large sudden shifts in wind direction that are unrelated to local turbulence (Mahrt 2008). These low-level fluctuations can even lead to measurable transport upwind from the mean direction (Mahrt et al. 2008). Dataset analysis suggests such wind fluctuations in the SBL are dominated by features in the *mesogamma* (2-20 km) and *sub-meso* (20-2000 m) scales (Mahrt 2009a). While Mahrt (2008) discusses numerous processes contributing to SBL wind fluctuations, including density currents over sloping terrain, internal gravity waves, and low-level jets (LLJs), their physics remains poorly understood.

This study continues recent DTRA-sponsored sub-kilometer numerical research at Penn State investigating SBL predictability. We hypothesize that a high-resolution NWP model with advanced numerics and minimal diffusion may enable simulation of at least the statistics of mesogamma-scale wind variance in the SBL (Gaudet et al. 2008). In this study a nested-grid model is used to simulate real cases of weakly forced flows in the nocturnal SBL over central PA, including sub-meso and mesogamma scale wind fluctuations on time scales of 20-120 min. Case studies and multi-case composites are used to investigate the model's predictive characteristics for the mean and fluctuating wind in the SBL. While model evaluation must span all scales from the synoptic scale to the plume scale, here we shall focus primarily on the sub-meso and mesogamma scales, neither of which is resolved by the standard synoptic meteorological data.

* *Corresponding author address*: Nelson L. Seaman, Penn State Univ., Dept. of Meteorology, University Park, PA 16802; e-mail: stauffer@meteo.psu.edu

2. NUMERICAL MODEL AND EXPERIMENT DESIGN

The model chosen for this research is the Weather Research and Forecasting (WRF) system's Advanced Research WRF (ARW) version 2.2.1 (Skamarock et al. 2005). ARW is configured with four nested domains having grids of 12-, 4-, 1.333- and 0.444-km (Fig. 1), each having a one-way interface with the next smaller grid. The innermost domain covers ~67 X 67 km centered on the Nittany Valley of central PA (Fig. 2). This region is dominated by narrow quasi-parallel ridges oriented southwest-to-northeast, which flank broad deep valleys. A portion of the Allegheny Mts. are located in the northwest part of the small domain. The 1.333-km domain covers ~256 X 224 km, encompassing almost the entire Allegheny Mts., but it only partly resolves the narrow ridge-and-valley topography of Central PA.

Two sets of model experiments are designed to explore the accuracy of SBL predictions as a function of (1) horizontal and vertical resolution and (2) SBL turbulence physics. Conditions for the grid-resolution experiments are given in Table 1. In Exp. Baseline all four domains have 43 layers, with 11 layers in the lowest 68 m above ground level (AGL) (Fig. 3a). The lowest 5 layers in this high-resolution configuration have thicknesses of 2 m each, after which the layer depths gradually increase with height up to the model top at 50 hPa. The very fine vertical resolution near the surface is designed to resolve SBL structure and its dominant physical processes. In Exp. LrgDZ the region below 68 m AGL is consolidated into just two layers (Fig. 3b), representing more conventional near-surface layer thicknesses. The total number of layers in Exp. LrgDZ is 34. Since both vertical-layer configurations have the same four horizontal domains, Exps. LrgDX and LrgDXDZ are easily represented by the 1.333-km solutions of the first two experiments. All the resolution-sensitivity experiments are run with the WRF's standard Mellor-Yamada-Janjic (MYJ) turbulence scheme (Janjic 2002), the Dudhia radiation scheme, simple ice physics and the five-layer soil model.

Exper. Name	Horiz. Grid (km)	Sfc. Layer Depth (m)	Layers Below 68 m
Baseline	0.444	2	11
LrgDZ	0.444	30	2
LrgDX	1.333	2	11
LrgDXDZ	1.333	30	2

Table 1. Design for the Baseline Exp. and three additional resolution-sensitivity experiments.

The second set of experiments explores sensitivity to the turbulence physics (Table 2). The first two experiments compare solutions using WRF's standard versions of the MYJ scheme (Exp. MYJstd) and the newer Quasi-Normal Scale Elimination turbulence scheme (Exp. QNSEstd) (Sukoriansky et al. 2006). For very stable conditions, stability can become so strong that the turbulence collapses (flow effectively becomes laminar). However, in a model at least some mixing is required to maintain numerical stability, which generally is specified through one or more constant parameters. Since the QNSE scheme in WRF borrows much of the code in the MYJ 1.5-order TKE-predicting scheme, both turbulence parameterizations contain similar minimum parameters: a background value of turbulent kinetic energy, TKE_{MIN}, and a limiting length scale, l_B. However, as shown in Table 2, while Exp. QNSEstd uses the same l_B as Exp. MYJstd, the TKE_{MIN} in Exp. QNSEstd is an order of magnitude smaller. Indeed,

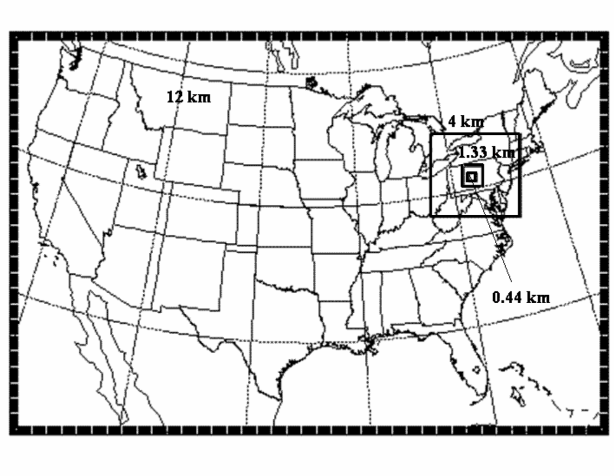

Figure 1. WRF four-domain nested grid configuration.

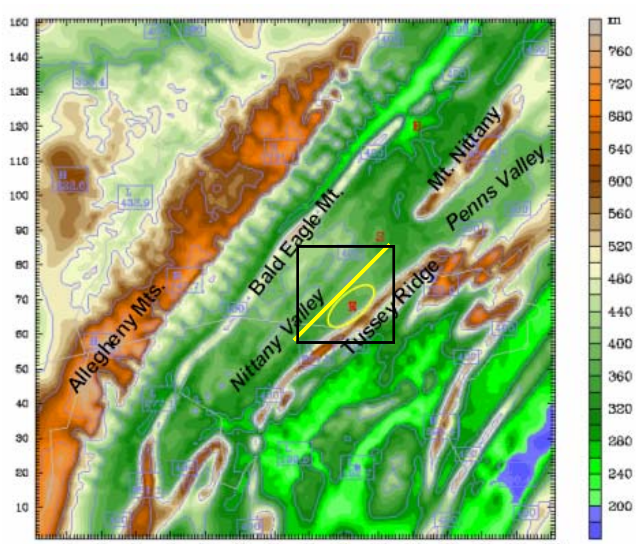

Figure 2. Topography of WRF on Domain 4, horizontal resolution 444 m. Oval marks site of local obs network.

testing has shown that the default values of these parameters in Exp. MYJstd may be too large for very stable conditions. Therefore, Exp. MYJmod uses the smaller TKE_{MIN}, similar to Exp. QNSEstd. To be consistent, though, the value of l_B also should be reduced by a factor of $(10)^{1/2}$ when TKE_{MIN} is reduced by 10. This is done in Exp. MYJmod.

All WRF forecast are run for 12 h during the nocturnal period, beginning at 0000 UTC. With a time step on the innermost domain of 2.5 s, each 12-h forecast takes ~6 h on four nodes of a Penn State Linux cluster, each node having four 3-GHz CPUs. Output files for the entire 1.333- and 0.444-km domains are saved at 12-minute intervals. Model data are saved over the local observing network at 10-s intervals to support analysis of sub-meso and mesogamma-scale fluctuations. Model evaluations are conducted using standard statistical analysis of individual and multiple-case composites. The potential impact on plume behavior is also evaluated for selected cases by calculating trajectories of parcels released in the SBL.

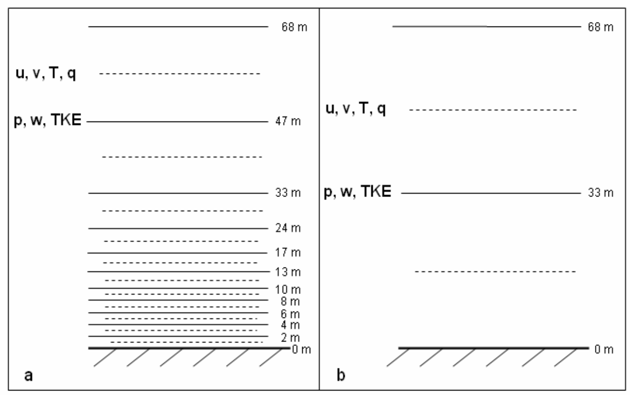

Figure 3. WRF-ARW vertical configurations below 68 m AGL. Baseline configuration shown in (a); conventional vertical-resolution configuration shown in (b).

Exper. Name	Physics Scheme	TKE_{MIN} (m^2s^{-2})	l_B (m)
MYJstd	MYJ	0.10	0.32
QNSEstd	QNSE	0.01	0.32
MYJmod	MYJ	0.01	0.10

Table 2. Design for turbulence-physics sensitivity experiments.

3. CENTRAL PA OBSERVING NETWORK

The sub-kilometer WRF domain described above is needed to resolve the fine-scale terrain in Central PA expected to drive near-surface drainage winds, internal gravity-wave propagation and vertical structure of the SBL. To evaluate the model's predictions at this scale, a local network of instrumented towers was deployed in a gently rolling section of Nittany Valley near Rock Springs, close to the northwest base of Tussey Ridge (yellow ellipse, Fig. 2). Stauffer et al. (2009) describes the fast-response instrumentation that provide wind and temperature measurements from the network.

4. MODEL RESULTS AND EVALUATION

4.1 *Evaluation on Coarse Domains*

Before evaluating local solutions in the SBL on the model's inner domains in central PA, we examine the accuracy of WRF's predictions in Exp. Baseline at the synoptic and mesoalpha scales. Domain-wide statistical evaluation was performed for winds and temperatures using the Model Evaluation Toolkit (MET) code supported by the WRF Development Testbed Center (DTC) in Boulder, CO. Penn State has extended MET to provide statistics for wind direction. Scripted to run nightly following each model cycle, MET validates forecasts on the two outer domains against standard surface METAR and sonde data. For example, Figs. 4 and 5 present profiles of root mean square errors (RMSE) and bias errors (BE) for wind speed and direction at 1200 UTC for a composite of nineteen cases that favor SBL development in Oct-Nov 2007. Recalling that the 12-km domain covers the full CONUS, we note these errors generally are smaller than winter season-averaged forecast errors reported for a 5-km CONUS domain (Koch and Gall 2005).

4.2 *Evaluation on Local Domains*

On the local scale, the WRF model predictions are verified against 3-m and 9-m tower data from the field network at Rock Springs. Using one-minute averaged time series, Gaudet et al. (2008) and Stauffer et al. (2009) showed that both model and observed winds contain large fluctuations at a range of frequencies, but all are too low to be associated with the weak turbulence in the SBL. It is these sub-meso fluctuations that cause most of the erratic plume transport commonly found in weak-wind SBL cases. Next, they applied a 2-h running mean filter to the time series to isolate the more-predictable lower-frequency components (periods ~0.3-2.0 h) for statistical evaluation. This procedure removes the higher-frequency components found to be mostly non-deterministic in terms of their poor correlation with observed fluctuations at the same time scales (Gaudet 2008). We hypothesize that the retained large, lower-frequency fluctuations are associated primarily with near-surface cool drainage winds and the passage of mid-level internal gravity waves.

Using the filtered time series, the importance of enhanced horizontal and vertical grid resolution can easily be seen in the model's wind speed predictions for the case of 7 Oct. 2007 (Fig. 6). Recalling that all four of the model-resolution experiments use the standard MYJ scheme, it is evident that the combination of high vertical and horizontal resolution is necessary for the best prediction relative to the observations. All runs have a positive bias, but the 9-m wind speed forecast is especially sensitive to increased horizontal resolution.

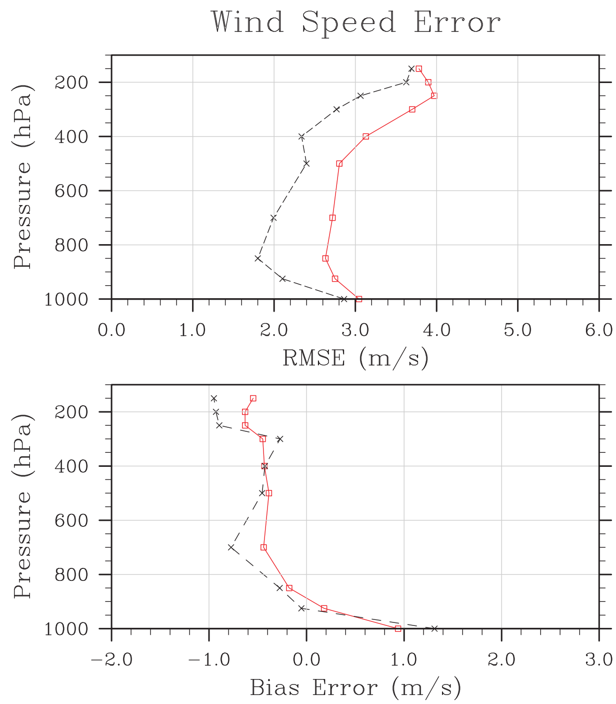

Figure 4. Nineteen-case composite of RMSEs (top) and bias errors (bottom) for wind speed in 12-h WRF forecasts for autumn 2007 on12-km CONUS (red solid) and 4-km regional domains (black dashed).

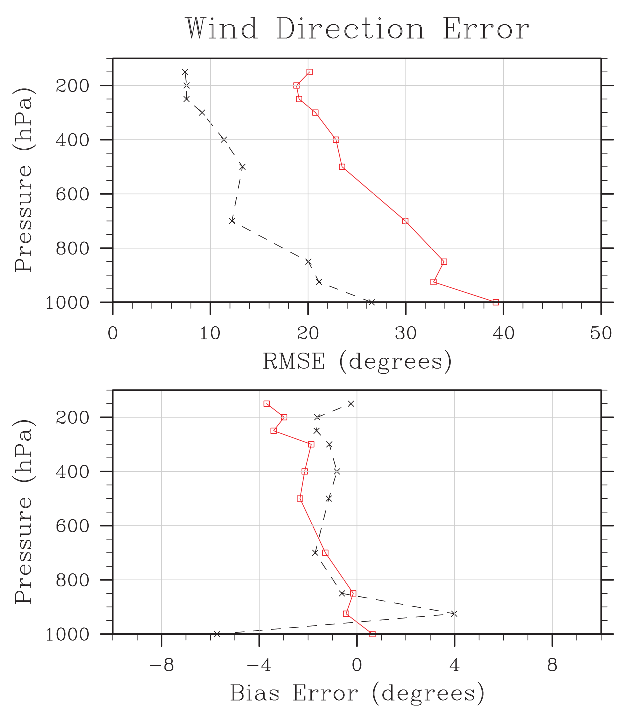

Figure 5. Same as Fig. 4, but for composite RMSEs (top) and bias errors (bottom) for wind direction.

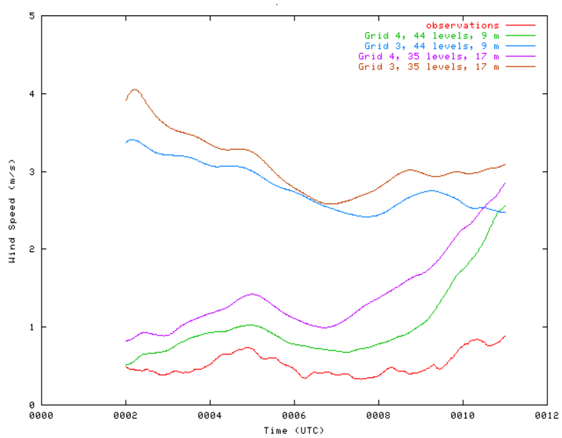

Figure 6. Comparison of filtered time series of observed and modeled wind speed (ms^{-1}) at 9 m AGL, Rock Springs, PA, for the period 0000-1200 UTC, 7 October 2007. The lowest curve (red) represents observations, followed by model experiments in order of increasing speed: Exps. Baseline (green), LrgDZ (magenta), LrgDX (blue) and LrgDXDZ (brown).

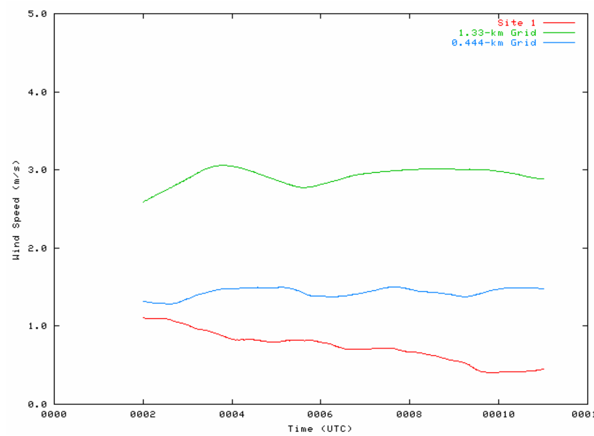

Figure 7. Filtered time series of wind speed (ms^{-1}) in nocturnal SBL at 9 m AGL, composited over 16 autumn cases. Shown are observed speed (red) versus Exp. Baseline 0.444-km grid (blue) and Exp. LrgDX 1.33-km grid (green).

A similar result was found when the running-mean filter was applied to 16 cases from Oct-Nov 2007 having very strong nocturnal SBLs. Figure 7 shows the composite of filtered time series for wind speed at 9 m AGL. It is apparent that Exp. Baseline predicts the very weak observed wind speeds reasonably well on the 0.444-km domain (small bias), but the 1.333-km grid (Exp. LrgDX) produces a much larger bias, similar to the single case in Fig. 6. It is hypothesized that much of the model's failure to simulate the gradually decreasing speeds observed through the night may be due to the behavior of the MYJ PBL scheme in very stable conditions, related to its minimum parameters (Table 2).

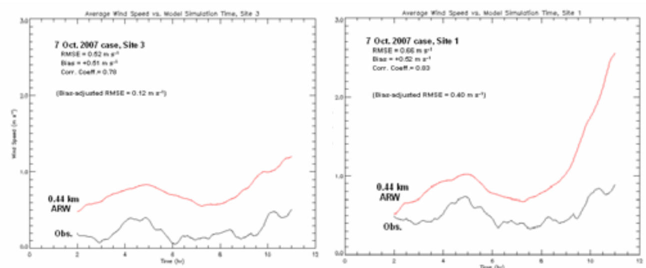

Figure 8. Comparison of filtered observed (black) and modeled (red) wind speed (ms^{-1}) for Exp. MYJstd at Rock Springs, PA, for 0000-1200 UTC, 7 Oct. 2007: (left) 3 m AGL, (right) 9 m AGL.

Next, we evaluate the sensitivity of WRF solutions to the turbulence physics. First, Fig. 8 compares time series of observed versus model-predicted wind speed at 3 m and 9 m AGL in Exp. MYJstd for the case of 7 Oct. 2007, revealing shear in the lowest 10 m and positive biases. Figure 9 compares the 3-m winds in Exps. MYJmod and QNSEstd for the same case. Statistics for 3-m winds in all three experiments are given in Table 3. As in Figs. 6 and 7, it is apparent that Exp. MYJstd has a systematic positive BE that contributes significantly to its RMSE. Nevertheless, there is good correlation between the observations and the model-predicted time series in Exp. MYJstd. Use of the smaller limiting parameters in Exp. MYJmod reduces the speed bias at 3 m AGL by ~60% for this case (Table 3). The table also shows slightly larger errors for 3-m wind in Exp. QNSEstd, compared to Exp. MYJmod, at least for this case. Statistics from a second case, 3 Nov. 2007, are also shown in Table 3 for Exps. MYJstd and MYJmod, but none are available for Exp. QNSEstd at this time.

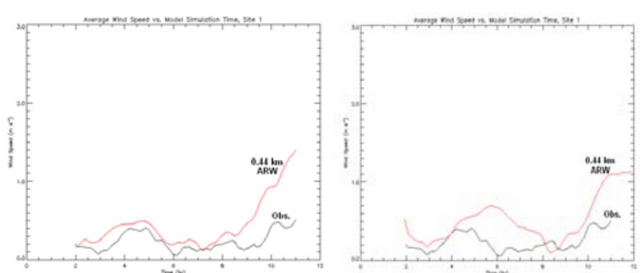

Figure 9. Comparison of filtered (observed) and modeled (red) wind speed (ms^{-1}) at 3 m AGL, Rock Springs, PA, for 0000-1200 UTC, 7 Oct. 2007: (left) Exp. MYJmod, (right) Exp. QNSEstd.

The vertical structure of several critical variables in the lowest 100 m is examined in Figs. 10-13. Since the data currently available from the Rock Springs network are limited to 3 m and 9 m AGL, we can only conduct qualitative evaluation of the profiles at this time.

	7 October 2007			
Exp.Name	BE	RMSE	$RMSE_{BA}$	Corr.Cof.
MYJstd	0.48	0.51	0.18	0.77
QNSEstd	0.23	0.30	0.20	0.59
MYJmod	0.22	0.33	0.25	0.80
	3 November 2007			
	BE	RMSE	$RMSE_{BA}$	Corr.Cof.
MYJstd	0.38	0.45	0.25	0.77
MYJmod	0.34	0.40	0.22	0.82

Table 3. Statistics for model-predicted wind speed (ms^{-1}) at 3 m AGL in turbulence-sensitivity experiments (see Table 2). BE = bias error, RMSE = root mean square error, $RMSE_{BA}$ = bias adjusted RMSE, Corr. Cof. = correlation coefficient.

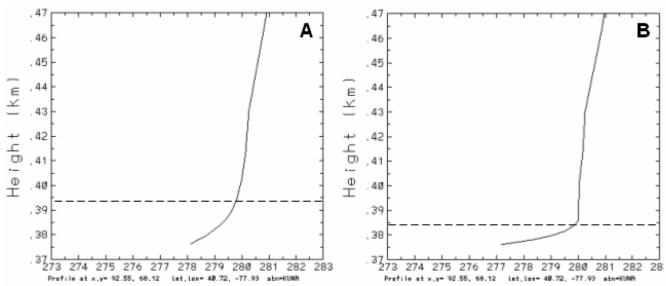

Figure 10. Vertical profile of θ (K) predicted by WRF in lowest 100 m AGL at Rock Springs, PA, 0400 UTC, 3 Nov. 2007. (a) Exp. MYJstd, (b) Exp. MYJmod. Dashed line is diagnosed SBL depth.

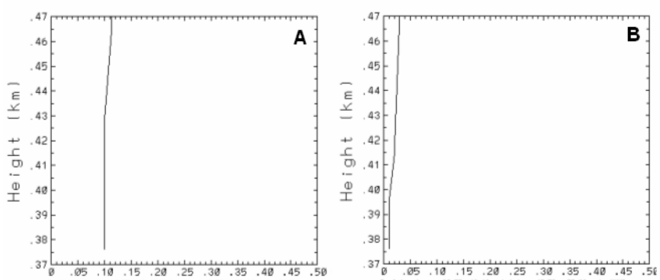

Figure 11. Same as Fig. 10, except for TKE (m^2s^{-2}) (a) Exp. MYJstd, (b) Exp. MYJmod.

However, the WRF model results are consistent with published field data and other modeling studies (e.g., Steeneveld et al. 2006). First, for the 3 Nov. case, Figure 10 shows WRF-predicted potential temperature (θ) profiles with very stable, shallow BLs in Exps. MYJstd and MYJmod, but the surface temperatures are colder in Exp. MYJmod, the SBL is shallower and the near-surface stability is greater than in Exp. MYJstd. This is consistent with the result in Table 3 that showed a reduced warm bias at 3 m in Exp. MYJmod. Figure 11 shows the corresponding profiles of *TKE* in the same experiments, which reveal turbulence has collapsed in the SBL to the specified background minimums, TKE_{MIN}. However, while the *TKE* profile in Exp. MYJstd remains at the background value through most of the lowest 100 m, the *TKE* quickly becomes greater than TKE_{MIN} above the SBL in Exp. MYJmod and gradually grows larger with height in the less stable overlying air mass. Figure 12 shows the wind speed in Exp. MYJmod develops a characteristic slight LLJ at the top of the SBL and surface winds of ~0.3 ms^{-1}, while the LLJ in Exp. MYJstd is less distinct and surface winds are greater, ~0.6 ms^{-1}, reflecting the positive speed bias of this experiment. Lastly, Fig. 13 compares the corresponding θ-profiles predicted for Exps. MYJmod and QNSEstd in the 7 October case. As for the 3 Nov. case, the θ-profile in Fig. 13a develops a strong shallow inversion in the SBL, while in Fig. 13b, the inversion top is less distinct in Exp. QNSEstd (with the same value of TKE_{MIN}). Exp. QNSEstd also has a 2-m temperature that is colder by ~2 C. However, this result cannot be considered significant until more detailed evaluations are done using data from taller towers and many cases.

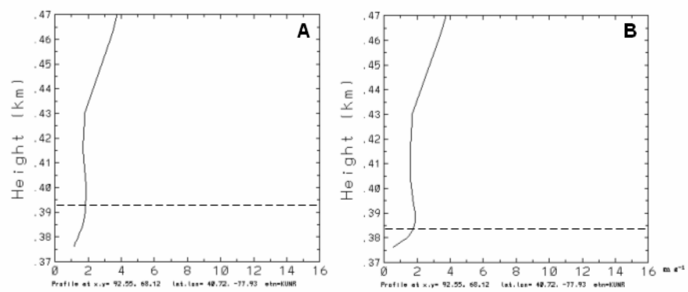

Figure 12. Same as Fig. 10, except for wind speed (ms^{-1}). (a) Exp. MYJstd, (b) Exp. MYJmod. Dashed line is diagnosed SBL depth.

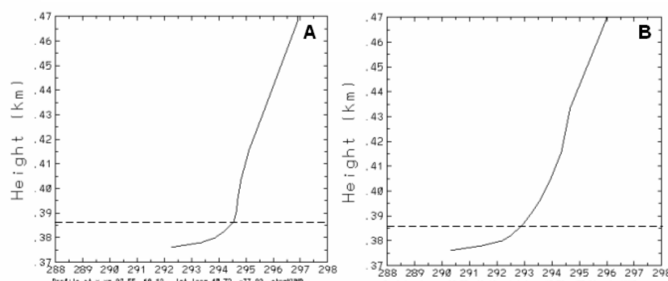

Figure 13. Vertical profile of θ (K) predicted by WRF in lowest 100 m AGL at Rock Springs, PA, 0800 UTC, 7 Oct. 2007. (a) Exp. MYJmod, (b) Exp. QNSEstd. Dashed line is diagnosed SBL depth.

Although the higher-frequency fluctuations filtered from the model-predicted time series in Figs. 6-9 have low correlation with observed fluctuations (not shown), Gaudet et al. (2008) found them to have similar spectra for time scales of ~20-120 minutes. At these time scales, the sub-meso motions can contribute significantly to plume transport in the SBL. Insight into the role of these high-frequency wind fluctuations can be gained by examining parcel trajectories based on WRF winds, without adding turbulent dispersion generated by an AT&D model. Figure 14 displays 3-h trajectories for nine parcels released in one 0.444-km grid cell at Rock Springs at 3 m AGL, 0800 UTC, 3 Nov. 2007. Using winds from Exp. MYJstd and without sub-grid dispersion (Fig. 14a), the cluster of parcels moves toward the northeast carried by mean southwesterly wind (~1 ms^{-1}) in the SBL. This direction is consistent with the most frequent directions observed in the valley. However, due to the periodic fluctuations in wind direction, many parcels move in a sinusoidal pattern characteristic of a classic stable meandering plume. As expected in real cases, this behavior is not universal. Some parcels released in the same grid cell exhibit weaker oscillatory behavior as they travel toward the northeast.

Figure 14b reveals similar near-surface trajectories in Exp. MYJmod, but because of its smaller minimum parameters, the trajectories exhibit greater dispersive behavior as the mean wind becomes weaker, allowing sub-meso components to dominate. In contrast, Fig. 14c shows trajectories from Exp. LrgDZ, which uses the standard MYJ scheme, but has only conventional vertical resolution. The coarser lower layers lead to significantly weaker gravity-driven downslope flows, thus damping sub-meso motions. This results in parcels traveling at faster speeds and with mostly straight-line trajectories. Finally, comparison of Figs. 14b and 14d indicates that the parcels experience weaker sub-meso motions (less meandering) and faster mean winds in Exp. QNSEstd than in Exp. MYJmod.

5. SUMMARY

In this study, an instrumented field network and a specially configured version of WRF-ARW have been used to study predictability of SBL structure and transport. It has been shown that sub-kilometer horizontal resolution and correspondingly fine vertical resolution are important for predicting the nocturnal SBL, including realistic profiles of TKE, θ, and wind speed. Additional experiments showed significant differences in WRF solutions in the SBL as a function of the turbulence physics of the MYJ and QNSE schemes. In particular, vertical structure of the predicted SBL in very stable conditions was strongly affected by the minimum parameters TKE_{MIN} and l_B. Potentially important differences appear in trajectories based on model solutions with the MYJ and QNSE schemes, but more detailed evaluations over many cases will be needed to understand these differences.

Acknowledgements: This research has been sponsored by the Defense Threat Reduction Agency under contract no. W911NF-06-1-0439-MOD-P00001. The Development Testbed Center in Boulder, CO, provided assistance with its MET codes.

6. REFERENCES

Gaudet, B.J., 2008: Definitions of determinism. 9th WRF Users' Workshop, Boulder, 23-27 June, 4 pp.

Gaudet, B.J., N.L. Seaman, D.R. Stauffer, S. Richardson, L. Mahrt, and J.C. Wyngaard, 2008: Verification of WRF-predicted mesogamma-scale spectra in the SBL using a high-frequency filter decomposition. 9th WRF Users' Workshop, Boulder, 23-27 June, 4 pp.

Janjic, Z.I., 2002: Nonsingular implementation of the Mellor-Yamada Level 2.5 Scheme in the NCEP Meso model. NCEP Office Note 437, 61 pp. Available online at http://www.ncep.noaa.gov.

Koch, S.E. and R. Gall, 2005: The DTC Winter Forecast Experiment: Final Project Report. Available from Development Testbed Center, Boulder, CO, 27 pp.

Mahrt, L., 2008: Mesoscale wind direction shifts in the stable boundary-layer. *Tellus*, **60A**, 700-705.

Mahrt, L., 2009: Characteristics of submeso winds in the stable boundary layer. *Bound-Layer. Meteor*., **130**, 1-14.

Mahrt, L., D. Stauffer and N. Seaman, 2008: Analysis of observed wind variability in the stable boundary layer using meso-networks. *Chem. Bio. Def.: Phys. Sci. & Tech. Conf.*, New Orleans, LA, 17-21 November, 3 pp.

Skamarock, W.C., J.B. Klemp, J. Dudhia, D.O. Gill, D.M. Barker, W. Wang and J.G. Powers, 2005: A description of the advanced research WRF version 2. NCAR Tech. Note NCAR/TN-468+STR, 88 pp.

Stauffer, D.R., B.J. Gaudet, N.L. Seaman, J.C. Wyngaard, L. Mahrt, and S. Richardson, 2009: Sub-kilometer numerical predictions in the nocturnal stable boundary layer. AMS 23rd WAF/19th NWP Conf., Omaha, 1-5 June, 8 pp.

Steeneveld, G.J., B.J.H. Van de Wiel and A.A.M. Holtslag, 2006: Modeling the evolution of the atmospheric boundary layer coupled to the land surface for three contrasting nights in CASES-99. *J. Atmos. Sci*., **63**, 920-935.

Sukoriansky, S., B. Galperin and V. Perov, 2006: A quasi-normal scale elimination model of turbulence and its application to stably stratified flows. *Nonlinear Proc. Geophys*., **13**, 9-22.

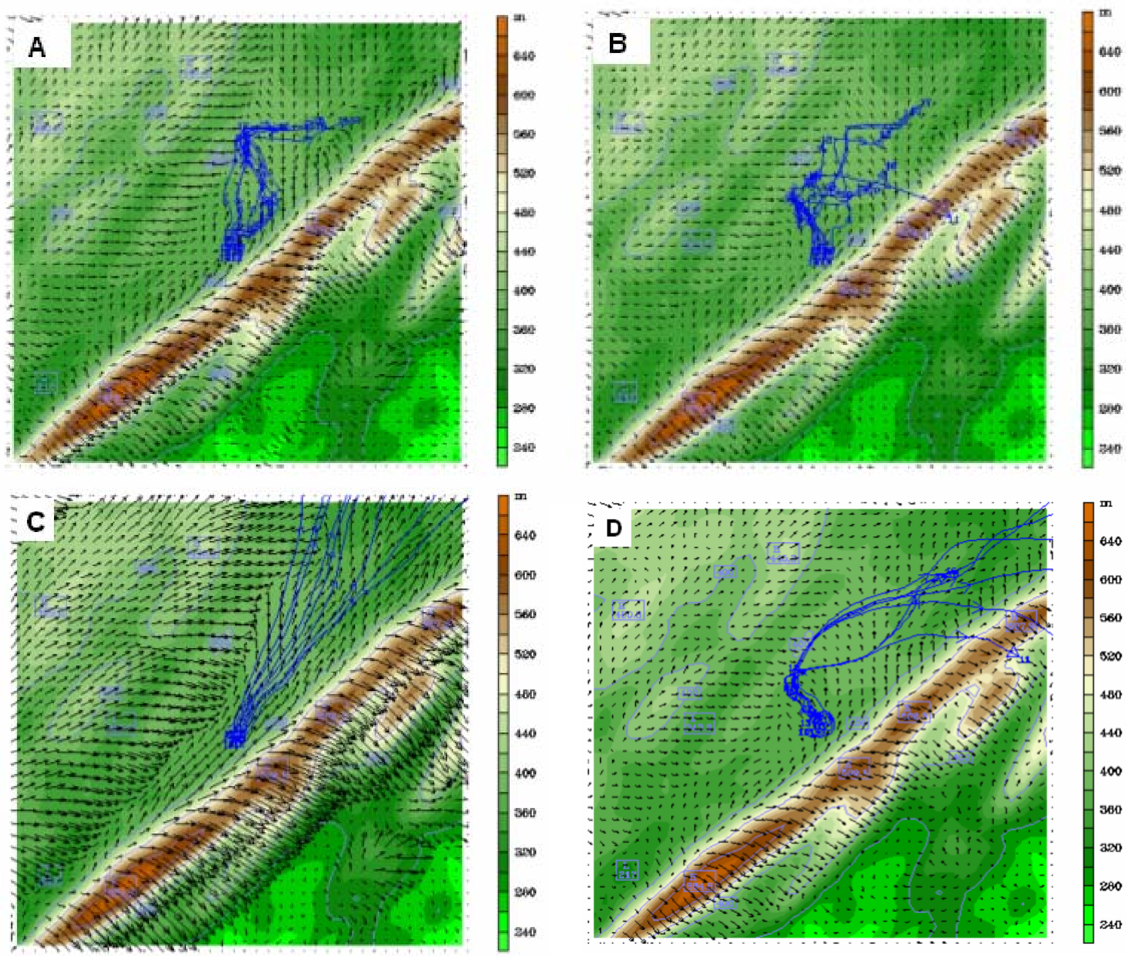

Figure 14. Parcel trajectories and WRF-predicted winds in the vicinity of Rock Springs, Nittany Valley, 0800-1112 UTC, 7 October 2007. Nine parcels are released at 3 m AGL in a 0.444 X 0.444 km area at 0800 UTC. (a) Exp. MYJstd, (b) Exp. MYJmod, (c) Exp. LrgDZ (uses standard MYJ scheme), (d) Exp. QNSEstd. Sub-domain location shown in Figure 3.